Trace moisture measurement in natural gas mixtures with a single calibration for nitrogen background gas

OPEN ACCESS
IOP Publishing
Measurement Science and Technology
Meas. Sci. Technol. **31** (2020) 104007 (7pp)
https://doi.org/10.1088/1361-6501/ab94ff

Trace moisture measurement in natural gas mixtures with a single calibration for nitrogen background gas

N Takeda[1], P Carroll[2], Y Tsukahara[1], S Beardmore[2], S Bell[2], K Yamanaka[1] and S Akao[1]

[1] Ball Wave Inc., Sendai, Japan
[2] National Physical Laboratory, Teddington, United Kingdom

E-mail: tsukahara@ballwave.jp

Received 26 October 2019, revised 13 May 2020
Accepted for publication 20 May 2020
Published 24 July 2020

Abstract

The measurement and control of trace moisture is an important procedure to maintain and secure the quality and safety of pipeline systems for natural gas. The natural gas mix typically comprises methane, ethane, propane, some higher hydrocarbons, carbon dioxide and nitrogen. It is too impractical to perform additional calibrations of trace moisture measurement every time the combination of gas components in the natural gas mix is changed. This paper proposes a method to separate and compensate for the effect of the background gas composition from the trace moisture measurement by using two different frequencies in a trace moisture analyzer utilizing a ball surface acoustic wave (SAW) sensor. The experiment was performed by connecting the ball SAW trace moisture sensor to supplies of trace moisture in multiple background gases from the National Physical Laboratory (NPL) Multi-gas, Multi-pressure Standard Humidity Generator, and changing the composition of the background gases including N_2, air, CH_4, 80% CH_4/20% C_2H_6, and 50% CH_4/50% C_2H_6. At the nominal humidity frost-point values of −70 °C, −50 °C, −40 °C and −30 °C, the deviations due to the change of the background gases were within ±1 °C in frost point.

Keywords: humidity, dew point, trace moisture, natural gas, calibration, hygrometer

(Some figures may appear in colour only in the online journal)

1. Introduction

The measurement of trace moisture in natural gas mixtures is an important process for the quality management of pipeline systems for natural gases [1]. Various types of trace moisture analyzer [2] are used for monitoring the trace moisture in different types of gases. Cavity ring down spectroscopy (CRDS) achieved the lowest detection limit [3], but its application has been mostly to the trace moisture in high-purity gases while the natural gas mix typically consists of methane, ethane, propane, some heavier hydrocarbons, carbon dioxide and nitrogen. A chilled mirror hygrometer [4] has good long-term stability and reproducibility, and often high resolution, but response time is slow in the trace range, therefore it is suitable for calibration purposes but not for online measurement. Recently, a progress was made toward miniaturization of the chilled mirror hygrometer based on integrated photonics platform [5] but the low detection limit was larger than 1 part per million by volume (ppmv) and has to be improved. A capacitive sensor is of small size and mostly inexpensive, but in some applications such as in the natural gas mix, drift and long-term instability show up and response time is slow specifically in the trace range, although effort to improve its performance has been reported [6]. Tunable diode laser absorption spectroscopy (TDLAS) has been used for the trace moisture measurement in natural gas mixtures, but each of these gas components affects the measurement of trace moisture differently. Therefore, calibration is not so easy for

real-world applications where the mixture changes with time [7, 8], and the lowest detection limit has been 1ppmv, or sometimes higher [9]. Recently, a direct tunable diode laser absorption spectroscopy sensor was reported [10] for trace moisture measurements in methane, ethane, propane, and low CO_2 natural gas in the range of 0.31–25 000 ppmv. This may lead to a convenient system to perform trace moisture measurements in natural gas mix in this measurement range. Another interesting new proposal was reported [11] by utilizing metal–organic frameworks (MOFs) as the sensing material. The trace moisture measurement in sub-ppmv level in industrial gases such as nitrogen, argon, helium and oxygen was successfully reported but its applicability to natural gas mix is still an open question. Therefore, there is still a gap between the existing technologies of trace moisture measurement and the demand from industry: a technology platform that has a quick response compatible to the online measurement in natural gas mixture and in other industrial processes, that can be applied to various background gases with a single calibration, and that can be extended to measurements at very low detection limits of ppb-level.

Trace moisture analysers based on the principle of non-diffraction propagation of surface acoustic waves (SAWs) on a spherical solid object have been developed by Ball Wave Inc. [12, 13]. It has been shown that the trace moisture analyzer using the ball SAW sensor has a sub-ppb level of low detection limit and a quick response time [14]. It was found that the output of the analyser could be separated into two components, one corresponding to the trace moisture content and the other corresponding to the average molecular weight of the background gases [15]. The output corresponding to the trace moisture content was found to be approximately independent of the background gases. Based on this finding, the present article proposes that a single calibration method in nitrogen background gas can be applied to trace moisture measurements in a variety of natural gas mixtures using a ball SAW sensor: a candidate to fill the gap between the current technologies of trace moisture measurement and the demand from industry.

2. Measurement principle and experimental method

2.1. Trace moisture analyser utilizing ball SAW sensors

The ball SAW humidity sensor is a sorption type. The sensor consists of a single-crystal α-quartz, cut and polished into a spherical shape with a diameter of 3.3 mm as depicted in figure 1(a). The single-crystal α-quartz is a piezoelectric material that converts electrical signals to mechanical vibrations and vice versa. Electrodes were manufactured on the surface of the ball SAW sensor by depositing a metal thin film with a figure like a comb that is called an interdigital transducer (IDT). When electrical signals are fed into the IDT, a mechanical vibration of the surface is generated and propagates along the surface. This is called a Rayleigh wave [16]. Some of the present authors found that the Rayleigh wave could propagate along the spherical surface of a solid material for more than 100 turns [12, 13].

A thin layer of amorphous silica was deposited on the ball SAW sensor that has an ability to absorb and desorb

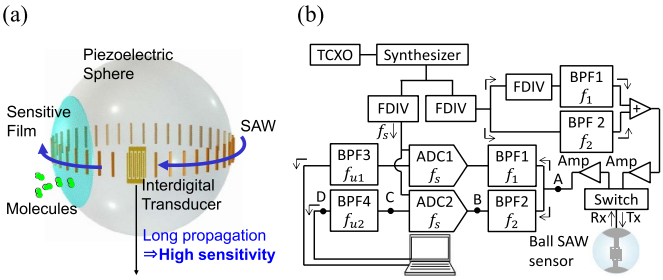

Figure 1. (a) The ball SAW sensor consists of a single-crystal α-quartz with IDT to generate surface acoustic wave (SAW) that propagates around the surface many times. The sensitive film selectively absorbs trace molecules such as H_2O. (b) A schematic of ball SAW trace moisture analyzer.

water molecules whereas the single-crystal α-quartz does not. If the ambient gas surrounding the ball SAW sensor contains water molecules some are absorbed in the amorphous silica layer. The elastic property of the layer changes because of the absorbed water molecules. This change of the elastic property affects the propagation of the Rayleigh wave in two ways: one is an increase of the velocity, and the other an increase of the attenuation. Hence, the amount of water molecules contained in the ambient gas can be estimated by measuring the changes either in the velocity or in the attenuation of the Rayleigh wave propagating around the surface of the ball SAW sensor [14]. Figure 1(b) shows the schematic diagram of the ball SAW trace moisture analyzer. A synthesizer driven by a stable signal source, TCXO, generates a radio-frequency signal that is divided into two different frequencies and fed to the IDT of the ball SAW sensor to generate the SAW propagation. The same IDT converts the SAW vibration to the electrical signal each time when the SAW propagating around the spherical quartz passes the IDT. The electrical signal contains two different frequency components, so that each frequency component is extracted by a bandpass filter and digitized by an analog-to-digital converter, and its amplitude is obtained as a function of the number of turns of the SAW propagation. In this way, the attenuation is measured for each of two frequency components. In section 2.2 we focus on the attenuation and detail its characteristic. Some more technical details of the ball SAW trace moisture analyzer can be found in [17].

2.2. A method to compensate for the difference in background gases in the calibration of trace moisture

The amount of water molecules sorbed by the sensor does not depend on the background gas composition. But the attenuation of the Rayleigh wave depends on the background gas composition, so that it should be compensated for as explained in the following. There are two mechanisms for the attenuation of the Rayleigh wave: one is a viscoelastic loss and the other a leakage loss (figure 2). The viscoelastic loss is caused by the energy dissipation of the vibration in materials, namely in the surface layer of amorphous silica containing water molecules. In the first-order approximation, the attenuation coefficient, or viscoelastic factor, α_V is proportional to the square of the vibration frequency, f. Another mechanism of attenuation is

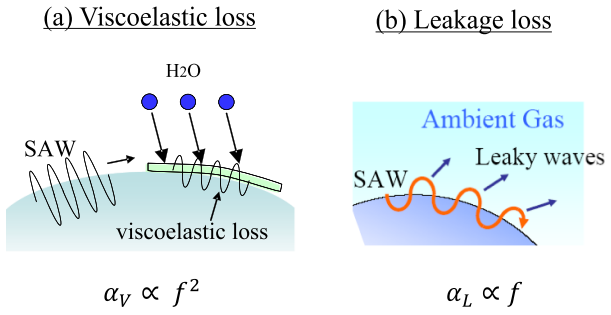

Figure 2. Two distinct mechanisms for the attenuation of surface acoustic waves, (a) the viscoelastic loss, α_V, in the solid materals is in proportion to the square of the frequency, f, (b) the leakage loss, α_L, due to the irradiation into the ambient gas is in proportion to the frequency, f.

due to the fact that a part of the vibration energy is transmitted into the surrounding background gas as the Rayleigh wave propagates along the surface. The attenuation coefficient, or leakage factor, α_L is approximately proportional to the frequency, f [18, 19]. Therefore, the total attenuation at the frequency, f, is

$$\alpha \sim \alpha_V + \alpha_L, \tag{1}$$

$$\sim af^2 + bf. \tag{2}$$

An ITD was designed and fabricated that could generate a Rayleigh wave containing two different frequency components: namely at a fundamental frequency $f_1 = 80$ MHz, and the other at a third harmonic frequency $f_3 = 240$ MHz $= f_1 \times 3$. Detecting with the same IDT and using bandpass filters, the attenuations at the fundamental and the third harmonic frequencies, α_1 and α_3, respectively could be obtained. Using the equations (1) and (2), we could extract α_L and α_V at f_1 as follows:

$$\alpha_1 = \alpha(atf_1) = af_1{}^2 + bf_1, \tag{3}$$

$$\alpha_2 = \alpha(atf_2) = af_2{}^2 + bf_2. \tag{4}$$

Because $f_2 = f_1 \times 3$, the equations (3) and (4) constitute a simultaneous linear equation for $af_1{}^2$ and bf_1. It is easily solved and since $bf_1 = \alpha_L(atf_1)$ and $af_1{}^2 = \alpha_V(atf_1)$:

$$\alpha_L(atf_1) = \frac{9\alpha_1 - \alpha_2}{6}, \tag{5}$$

$$\alpha_V(atf_1) = \frac{\alpha_2 - 3\alpha_1}{6}. \tag{6}$$

This extracted $\alpha_V(atf_1)$ contains only the effect of viscoelastic loss, and its change reflects the amount of water molecules absorbed in the surface layer, while the effect of the background gas is separated into the $\alpha_L(atf_1)$. Therefore, we could estimate the trace moisture content regardless of the difference in the background gas composition.

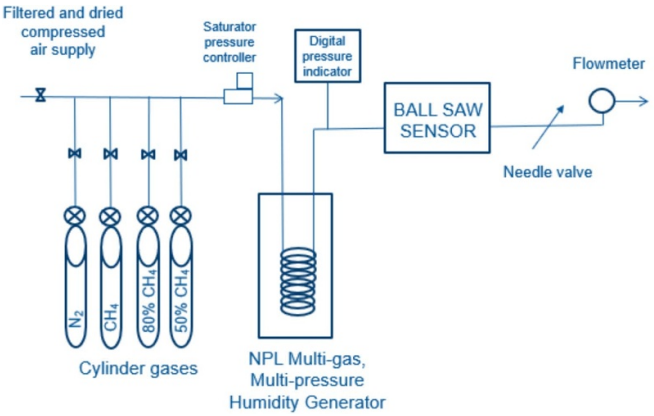

Figure 3. Calibration set-up for ball SAW sensor testing using NPL Multi-gas, Multi-pressure Standard Humidity Generator.

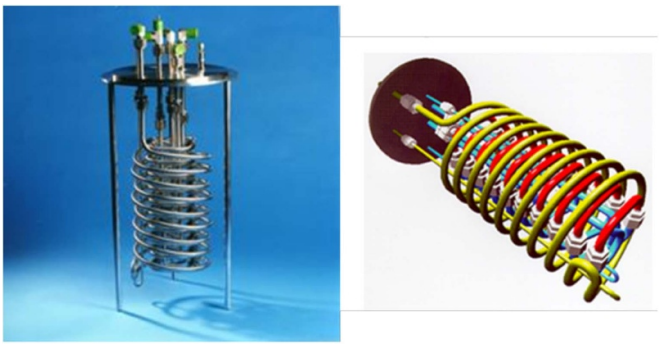

Figure 4. NPL multi-gas, multi-pressure standard humidity generator saturator for single gas species and gas mixtures at pressures up to 3 MPa.

2.3. Experimental set-up and NPL multi-gas, multi-pressure standard humidity generator for natural gas mixtures

In order to demonstrate the method, the SAW trace moisture analyser was connected to the Multi-gas, Multi-pressure Standard Humidity Generator at NPL (National Physical Laboratory) as shown in figure 3.

The humidity generator [20] comprises a flowing gas supply humidified by saturation with water vapour at defined temperature and pressure. In addition, saturated gas can be blended, if required, with dry gas to give a selected value of humidity and supplied to instruments under test.

The saturator coil, shown in figure 4, is located in an ethanol bath which is temperature-controlled by a circulation thermostat to maintain the required saturation temperature. Defined gas pressure is maintained using a pressure controller. As the gas thermally equilibrates, it becomes saturated with water vapour. The saturation temperature is measured using a platinum resistance thermometer (PRT) with traceability to national standards for temperature. The saturator is efficient such that this temperature defines the dew-point (or frost-point) temperature of the gas leaving the generator, to within a small uncertainty that has been characterised [21, 22] along with all other significant uncertainties, in a rigorous analysis. In this work, the facility was used in single-pressure mode,

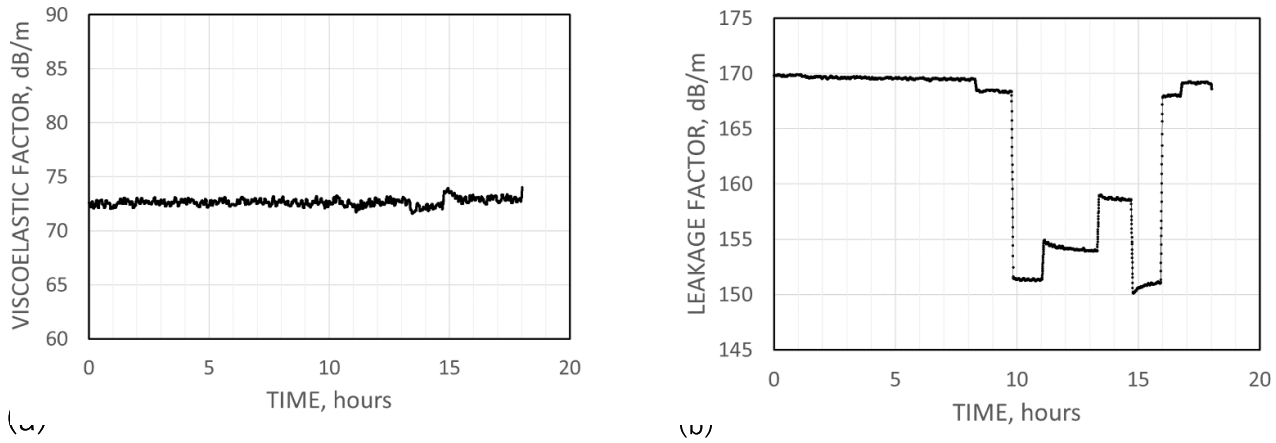

Figure 5. Quantity of total attenuation was separated in two factors: (a) viscoelastic factor, α_V, and (b) the leakage factor, α_L, through simple mathematics. The humidity generator produced a stable frost-point value of nominally −60 °C.

with no significant pressure changes, so that deviations from ideal gas behaviour would be negligible.

Test gas was supplied at just above atmospheric pressure (0.105 MPa or 1.05 bar). The gases used for the tests were nitrogen (N4.5), pure methane (N4.5), a pre-made mixture of nominally 80% methane and 20% ethane and a pre-made mixture of nominally 50% methane and 50% ethane (all supplied in cylinders) and NPL site-supplied compressed, filtered, dry air. The gas component actual fractions deviated by no more than 0.1% from nominal value, as reported in UKAS certificates of calibration of the gas mixture compositions. The uncertainty in actual value of each fraction was no more than 0.065% ($k = 2$). After saturation at the temperature of the generator, the gas was brought to room temperature of 23 °C ± 3 °C before passing to the sensor being tested, which was also at room temperature.

The generated humidity was set to a certain value, for example a frost point of −60 °C, and the background gas was switched in a sequence of air, N_2, CH_4, 80% CH_4/20% C_2H_6, 50% CH_4/50% C_2H_6, CH_4, N_2, and then air, while the attenuation coefficients of the ball SAW sensor were measured at the two frequencies. Each step in a sequence took one hour and the attenuation measurement was made at every 12 s. The stability during the sequence is shown in figure 5(a). The trace moisture in air was measured twice, at the beginning and the end of the sequence, to ensure the repeatability of the measurement. Then, the generated humidity was changed to the next value, for example a frost point of −50 °C, and the same procedure was repeated.

3. Results

3.1. Measured trace moisture

Figure 5 shows the extracted values of the viscoelastic factor $\alpha_V(atf_1)$ and the leakage factor $\alpha_L(atf_1)$, when the humidity generator produced the frost-point value of nominally −60 °C. In 5(a), values of the viscoelastic factor stay almost constant as expected. Small deviations are observed, too, which should be studied carefully in the future. In 5(b), the leakage factor shows a clear dependence on the change in the background gas contents. It can be shown that a mean molecular weight or a mean gas parameter of the background gas can be estimated from the leakage factor [15].

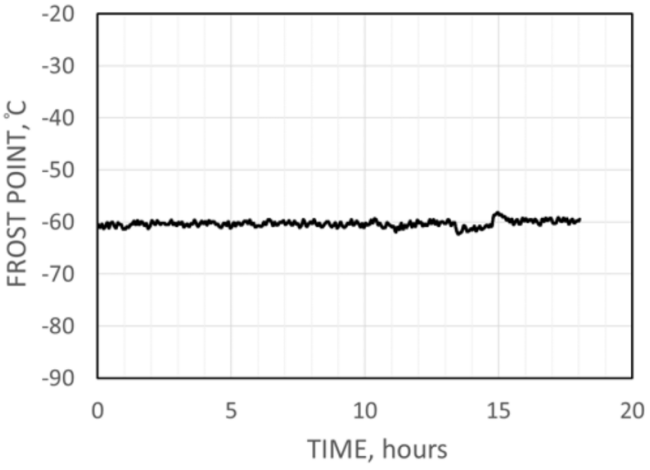

Figure 6. The values of frost point were calculated from the viscoelastic factor by using the calibration curve shown in figure 7. The humidity generator produced a stable frost-point value of nominally −60 °C for the duration shown.

We performed a calibration as described in section 3.2, so as to relate the viscoelastic factor to the values of trace moisture content. Referring to the calibration, we obtained the trace moisture content as shown in figure 6 while the humidity generator was set to a frost point of −60 °C and cycled through the background gases in the order described in section 2.3. The same experimental procedure was repeated while the humidity generator produced the nominal humidity frost-point values of −70 °C, −50 °C, −40 °C and −30 °C.

3.2. Calibration and results

A calibration was performed at target frost point values from the Multi-gas, Multi-pressure Standard Humidity Generator

Table 1. Summary uncertainty budget for calibrations in air, nitrogen and pure methane.

Uncertainty component	Standard uncertainty/°C at −70 °C	Standard uncertainty/°C from −60 °C to −30 °C
Saturator PRT temperature measurement	0.015	0.015
Saturation efficiency, temperature conditioning and pressure variations	0.074	0.054
Leaks, desorption and contamination	0.034	0.018
Instrument contributions: reproducibility, resolution, short-term stability	0.262	0.265
Combined standard uncertainty	0.275	0.271
Expanded uncertainty ($k = 2$)	0.550	0.542

Table 2. Uncertainty budgets for calibrations in 80% methane 20% ethane mixture.

Uncertainty component	Standard uncertainty/°C at −70 °C	at −60 °C	from −50 °C to −30 °C
Saturator PRT temperature measurement	0.015	0.015	0.015
Saturation efficiency, temperature conditioning and pressure variations	0.415	0.334	0.054
Leaks, desorption and contamination	0.034	0.034	0.018
Instrument contributions: reproducibility, resolution, short-term stability	0.262	0.265	0.265
Combined standard uncertainty	0.492	0.431	0.271
Expanded uncertainty ($k = 2$)	0.984	0.862	0.542

Table 3. Uncertainty budgets for calibrations in 50% methane 50% ethane mixture.

Uncertainty component	Standard uncertainty/°C from −70 °C to −60 °C	at −50 °C	from −40 °C to −30 °C
Saturator PRT temperature measurement	0.015	0.015	0.015
Saturation efficiency, temperature conditioning and pressure variations	0.594	0.415	0.054
Leaks, desorption and contamination	0.034	0.034	0.018
Instrument contributions: reproducibility, resolution, short-term stability	0.266	0.262	0.265
Combined standard uncertainty	0.652	0.492	0.271
Expanded uncertainty ($k = 2$)	1.30	0.984	0.542

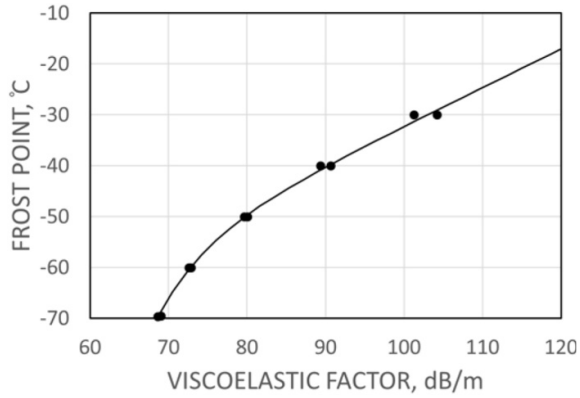

Figure 7. A calibration curve was obtained for nitrogen background gas, by feeding the nitrogen gas with predetermined values of target humidity produced by the NPL multi-gas multi-pressure standard humidity generator.

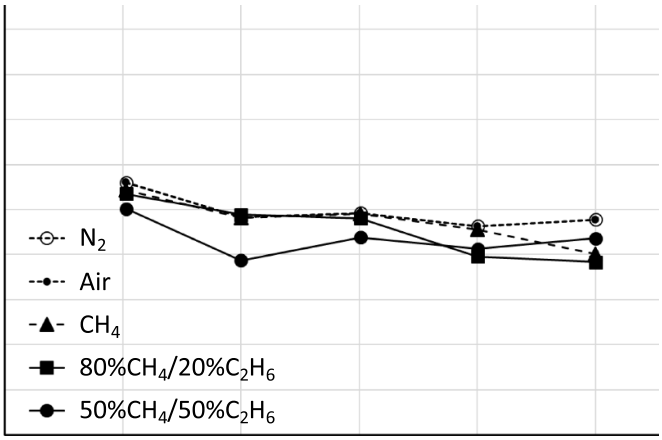

Figure 8. Error in the trace moisture measurements in different background gas mixtures using a single calibration in the nitrogen background gas shown in figure 7. Comparison was made in the gas mixtures; N_2, air, CH_4, 80% CH_4/20% C_2H_6, and 50% CH_4/50% C_2H_6. The deviations were within ± 1 °C. Lines are shown to guide the eye. Measurement uncertainties are given in section 4.1.

of − 70 °C, − 60 °C, − 50 °C, − 40 °C and − 30 °C while obtaining the viscoelastic factors in the nitrogen background gas. Figure 7 shows the calibration curve so obtained in the nitrogen background gas.

Then, the same calibration curve was applied to other background gases and mixtures and the resultant values of the trace moisture were compared to the reference humidity values. Figure 8 shows a graph of error (corrected instrument value minus generator reference value) versus nominal frost point,

for the different background gases and mixtures. In this humidity range, the errors are within ±1 °C in frost point. Hence, this verified that no additional calibrations are needed for most practical applications even if the combination of gas components in the background natural gas mix is changed. This is clear evidence that the ball SAW trace moisture analyser can obtain the correct trace moisture with a single calibration for nitrogen background gas even when the combination of the background gas components, such as methane, ethane, carbon dioxide and nitrogen, changes in the natural gas mixtures.

4. Discussion

4.1. Uncertainty

Calibration uncertainties were evaluated according to the approach in JCGM100 [23], and full details of this evaluation for NPL primary humidity standards have been published previously [21, 22]. The standard uncertainty of the generated frost point is calculated by combining the estimated uncertainties arising from the calibration, drift, self-heating and measurement of the PRTs, the saturation efficiency, temperature conditioning and pressure variations of the NPL Generator, the temperature variations in the generator bath and the effects of leaks, desorption and contamination. At −70 °C additional uncertainty was allowed for the operation of the generator below its formally validated lower limit (−60 °C). The standard uncertainty of measurement is calculated by combining the standard uncertainties of the generated dew point, the test hygrometer standard deviation, its resolution and an estimate of its reproducibility during calibration. The reported expanded uncertainty is based on a standard uncertainty multiplied by a coverage factor $k = 2$, providing a coverage probability of approximately 95%. A summary of the evaluation of uncertainty is given in tables 1 to 3 for the different background gases. In each table, the first three rows relate to the uncertainty in the generated humidity condition, and the fourth row summarises the uncertainty in the results due to the short-term performance of the sensor system during testing.

5. Conclusion

Trace moisture values in different mixtures of background gases representing the variation of components in natural gas mixtures were estimated using a ball SAW sensor with a single calibration for nitrogen background gas. It was established that the trace moisture analyzer utilizing the ball SAW sensor was able to obtain the correct values of trace moisture in different background gases including N_2, air, CH_4, 80% CH_4/20% C_2H_6, and 50% CH_4/50% C_2H_6 with a single calibration using nitrogen background gas. This was made possible because the impact of the change in the background gases on the ball SAW sensor moisture measurement could be eliminated by measuring two different frequency components at the same time.

The typical pressure range in the natural gas pipe-line is 1–7 MPa, but the experiment shown in this paper was performed at the atmospheric pressure. A further development is under way to cover the higher pressure.

ORCID iD

Y Tsukahara https://orcid.org/0000-0003-3729-8966

References

[1] ISO/TC 193/SC 1989—*ANALYSIS OF NATURAL GAS*—ISO 6327: 1981 *Gas Analysis—Determination of the Water Dew Point of Natural Gas—Cooled Surface Condensation Hygrometers* (International Organisation for Standardization)
[2] Abe H 2009 A marked improvement in the reliability of the measurement of trace moisture in gases *Synthesiology* **2** 223
[3] Hashiguchi K, Lisak D, Cygan A, Ciuryło R and Abe H 2016 Wavelength-meter controlled cavity ring-down spectroscopy: high-sensitivity detection of trace moisture in N2 at sub-ppb levels *Sens. Actuators* A **241** 152–60
[4] Wylie R G 1957 A new absolute method of hygrometry. I. the general principles of the method *Australian J. Phys.* **10** 351–65
[5] Tao J, Luo Y, Wang L, Cai H, Sun T, Song J, Liu H and Gu Y 2016 An ultrahigh-accuracy miniature dew point sensor based on an integrated photonics platform *Sci. Rep.* **6** 29672
[6] M R M, Z H Z and Islam T 2016 A sensitive and highly linear capacitive thin film sensor for trace moisture measurement in gases *Sens. Actuators* B **228** 658–64
[7] Stockwell P 2007 Tunable Diode Laser (TDL) systems for trace gas analysis *Measurement and Control* **40** 272–7
[8] Soleyn K 2009 Development of a tunable diode laser absorption spectroscopy moisture analyzer for natural gas *Proc. 5th Int. GAS Analysis Symp., GAS 2009* (*Rotterdam, the Netherlands, February 11–13*)
[9] Pal S, Das A, Nandy S, Kar R and Ghosh J 2019 Development of a near-infrared tunable diode laser absorption spectrometer for trace moisture measurements in helium gas *Rev. Sci. Inst.* **90** 103105
[10] J A N, Pratzle S, Werhahn O and Ebert V 2017 Tunable diode laser absorption spectroscopy sensor for calibration free humidity measurements in pure methane and low CO_2 natural Gas *Appl. Spectroscopy* **71** 888–900
[11] Ohira S, Nakamura N, Endo M, Miki Y, Hirose Y and Toda K 2018 Ultra-sensitive trace-water optical sensor with *in situ*-synthesized metal–organic framework in glass paper *Analytic. Sci.* **34** 495–500
[12] Yamanaka K, Cho H and Tsukahara Y 2000 Precise velocity measurement of surface acoustic waves on a bearing ball *Appl. Phys. Lett.* **76** 2797–9
[13] Tsukahara Y, Nakaso N, Cho H and Yamanaka K 2000 Observation of diffraction-free propagation of surface acoustic waves around a homogeneous isotropic solid sphere *Appl. Phys. Lett.* **77** 2926–8
[14] Takeda N and Motozawa M 2012 Extremely fast 1 μmol · mol^{-1} water-vapor measurement by a 1 mm diameter spherical SAW device *Int. J. Thermophys.* **33** 1642–9
[15] Yamanaka K, Akao S, Takeda N, Tsuji T, Oizumi T, Fukushi H, Okano T and Tsukahara Y 2019 Background gas analysis with leaky attenuation in a trace moisture analyzer using a ball surface acoustic wave sensor *Jpn. J. Appl. Phys.* **58** SGGB04

[16] Lord Rayleigh D C L, F R S 1885 On waves propagated along the plane surface of an elastic solid *Proc. London Mathematical Society* vol 12, pp 4
[17] Tsuji T, Oizumi T, Fukushi H, Takeda N, Akao S, Tsukahara Y and Yamanaka K 2018 Development of ball surface acoustic wave trace moisture analyzer using burst waveform undersampling circuit *Rev. Sci. Inst.* **89** 055006
[18] S J M, G C F and S D S 1994 Dynamics and response of polymer-coated surface acoustic wave devices: effect of viscoelastic properties and film resonance *Anal. Chem.* **66** 2201–19
[19] Slobodnik Jr. A J 1972 Attenuation of microwave acoustic surface waves due to gas loading *J. Phys. D: Appl. Phys.* **43** 2565
[20] Carroll P A and Bell S A 2019 The NPL multi-gas, multi-pressure standard humidity generator *Metrologia* (in preparation)
[21] Stevens M and Bell S A 1992 The NPL standard humidity generator: an analysis of uncertainty by validation of individual component performance *Meas. Sci. Technol.* **3** 943–52
[22] Stevens M 1999 The new NPL low frost-point generator *Proc. TEMPMEKO '99, 7th Int. Symp. on Temperature and Thermal Measurements in Industry and Science* (*Delft 1999*) pp 191–6
[23] JCGM 100: 2008 *Evaluation of Measurement Data—Guide to the Expression of Uncertainty in Measurement* (Sèvres: JCGM)